BIOMOLECULES & THERAPEUTICS

Original Article
Biomol Ther 30(4), 360-367 (2022)

Characterization of KRC-108 as a TrkA Kinase Inhibitor with Anti-Tumor Effects

Hyo Jeong Lee[1], Yeongyu Moon[2], Jungil Choi[2], Jeong Doo Heo[2], Sekwang Kim[1], Hari Krishna Nallapaneni[3], Young-Won Chin[4], Jongkook Lee[3] and Sun-Young Han[1,*]

[1]College of Pharmacy and Research Institute of Pharmaceutical Sciences, Gyeongsang National University, Jinju 52828,
[2]Gyeongnam Biohealth Research Center, Gyeongnam Branch Institute, Korea Institute of Toxicology, Jinju 52834
[3]College of Pharmacy, Kangwon National University, Chuncheon 24341,
[4]College of Pharmacy and Research Institute of Pharmaceutical Sciences, Seoul National University, Seoul 08826, Republic of Korea

Abstract

Tropomyosin receptor kinase A (TrkA) protein is a receptor tyrosine kinase encoded by the *NTRK1* gene. TrkA signaling mediates the proliferation, differentiation, and survival of neurons and other cells following stimulation by its ligand, the nerve growth factor. Chromosomal rearrangements of the *NTRK1* gene result in the generation of TrkA fusion protein, which is known to cause deregulation of TrkA signaling. Targeting TrkA activity represents a promising strategy for the treatment of cancers that harbor the TrkA fusion protein. In this study, we evaluated the TrkA-inhibitory activity of the benzoxazole compound KRC-108. KRC-108 inhibited TrkA activity in an *in vitro* kinase assay, and suppressed the growth of KM12C colon cancer cells harboring an *NTRK1* gene fusion. KRC-108 treatment induced cell cycle arrest, apoptotic cell death, and autophagy. KRC-108 suppressed the phosphorylation of downstream signaling molecules of TrkA, including Akt, phospholipase Cγ, and ERK1/2. Furthermore, KRC-108 exhibited anti-tumor activity *in vivo* in a KM12C cell xenograft model. These results indicate that KRC-108 may be a promising therapeutic agent for Trk fusion-positive cancers.

Key Words: Tropomyosin receptor kinase A, Neurotrophic receptor kinase 1 fusion, KRC-108, Colon cancer

INTRODUCTION

The tropomyosin receptor kinase (Trk) family consists of three members, TrkA, TrkB, and TrkC, which serve as receptors for neurotrophins (Reichardt, 2006). The neurotrophic receptor kinase (NTRK) genes *NTRK1*, *NTRK2*, and *NTRK3* encode the Trk proteins TrkA, TrkB, and TrkC, respectively (Khotskaya *et al*., 2017). TrkA was the first member of the Trk receptor family to be characterized, and binds to the nerve growth factor (NGF) ligand. The TrkA signaling pathway is similar to that of other receptor tyrosine kinases. Binding of NGF leads to dimerization and phosphorylation of TrkA, resulting in its activation. TrkA then phosphorylates and activates downstream signaling molecules such as phospholipase Cγ (PLCγ), phosphoinositol-3 kinase, and mitogen-activated protein kinase. NGF-TrkA signaling mediates the proliferation, differentiation, and survival of neurons and other cells.

NTRK1 gene fusions are known to cause deregulation of TrkA signaling. Chromosomal rearrangements involving the *NTRK1* gene result in the formation of TrkA fusion proteins with constitutively activated kinase activity. Fusion of TrkA with various protein partners induces dimerization independent of ligand binding. Several TrkA fusion protein partners have been identified, including tropomyosin 3 (TPM3), which results in the formation of the *TPM3-NTRK1* fusion (Martin-Zanca *et al*., 1986; Bongarzone *et al*., 1989). The resulting TPM3-TrkA fusion proteins are constitutively active, leading to oncogenesis. Since the discovery of *TPM3-NTRK1* fusion in colorectal cancer, TrkA activation resulting from gene fusion with various protein partners has been reported in multiple tumor types (Cocco *et al*., 2018). Trk fusion partners are presumed to affect dimerization, resulting in Trk kinase activation.

Inhibition of TrkA kinase activity is a promising strategy for cancer therapy based on the deregulated activity of TrkA ob-

Open Access **https://doi.org/10.4062/biomolther.2021.195**

Received Dec 28, 2021 **Revised** Feb 1, 2022 **Accepted** Feb 9, 2022
Published Online Mar 10, 2022

***Corresponding Author**
E-mail: syhan@gnu.ac.kr
Tel: +82-55-772-2423, Fax: +82-55-772-2429

served in several cancer types. Several TrkA inhibitors have been successfully developed as anticancer drugs. To date, the two Trk inhibitors, larotrectinib and entrectinib, were approved by the FDA in 2018 and 2019, respectively (Cocco *et al*., 2018). Larotrectinib and entrectinib were approved as tissue-agnostic agents, meaning that the drug can be indicated to patients with Trk fusion genes, independent of the tumor type. Development programs for next-generation Trk inhibitors are ongoing. Selitrectinib (LOXO-195) and repotrectinib (TPX-0005) are representative second generation Trk inhibitors in clinical development, and are designed to overcome the resistance observed with the first generation Trk inhibitors, larotrectinib and entrectinib (Harada *et al*., 2020). Diverse chemical scaffolds with Trk inhibitory function need to be characterized for next-generation inhibitors. To overcome the emergence of resistance and adverse effects of specific chemical scaffolds, more Trk inhibitors with various chemical structures need to be identified. In case of entrectinib, nervous system disorder, weight gain, and anemia are representative adverse effects (Doebele *et al*., 2020; Han, 2021).

This study aimed to characterize the inhibitory effect of the benzoxazole compound KRC-108 on TrkA kinase and its anti-tumor activities. KRC-108 was previously reported to be an inhibitor of c-Met, Flt3, and ALK (Han *et al*., 2012). Based on the kinase selectivity results, it is possible that KRC-108 can act as an anti-tumor agent by TrkA inhibition. Since the properties of the KRC-108 compound, including its pharmacokinetics, CYP450 inhibition, microsomal stability, and acute toxicity, are favorable for drug development, KRC-108 was characterized as an inhibitor of the cancer target TrkA. The inhibitory role of KRC-108 against TrkA kinase was evaluated using *in vitro* TrkA kinase activity and cell-based assays. KRC-108-mediated growth inhibition of cancer cells harboring the Trk fusion gene was examined both *in vitro* and *in vivo*. In addition, the downstream signaling of TrkA and the mechanism of cell growth inhibition were investigated.

MATERIALS AND METHODS

Compound

The design and synthesis of KRC-108 (3-(benzo[d]oxazol-2-yl)-5-(1-(piperidin-4-yl)-1H-pyrazol-4-yl)pyridin-2-amine) have been described previously (Cho *et al*., 2010). The compound was dissolved in dimethyl sulfoxide (DMSO) to a concentration of 10 mM and stored at –20°C.

In vitro kinase assay

A time-resolved fluorescence-based HTRF KinEASE-TK kit (Cisbio, Codolet, France) was used to evaluate TrkA kinase activity. Recombinant proteins containing the TrkA kinase domain were purchased from Invitrogen (Thermo Fisher Scientific, Waltham, MA, USA). The reaction was performed in a 96-well plate with a kinase reaction mixture containing 0.1 μM TK-substrate biotin, 500 μM ATP, and 1 ng of TrkA kinase with a 3-fold serial dilution of the test compound in kinase reaction buffer (50 mM HEPES [pH 7.0], 5 mM $MgCl_2$ 1 mM DTT, 0.1 mM orthovanadate, 0.01% bovine serum albumin [BSA], and 0.02% NaN_3). After addition of the detection reagents, the TR-FRET signal was measured with a Victor X5 multilabel reader (Perkin Elmer, Waltham, MA, USA) at 615 nm and 665 nm. An equal amount of 1% DMSO was added to each kinase reaction at every dose point. The dose-response curve was fitted by nonlinear regression, and the IC_{50} was calculated using Prism version 5.01 (GraphPad Software, San Diego, CA, USA).

Cell culture

The human colon cancer cell line KM12C was purchased from the Korean Cell Line Bank (Seoul, Korea). The cells were cultured in minimum essential medium (MEM; Thermo Fisher Scientific) supplemented with 10% fetal bovine serum (FBS) and 1% penicillin/streptomycin (Thermo Fisher Scientific) and maintained at 37°C in a humidified atmosphere with 5% CO_2.

KM12C cells were plated in a 96-well plate (2,000 cells/well) and incubated with KRC-108 for 72 h at 37°C. Three-fold serial dilutions of KRC-108 were prepared in DMSO to create a 10-point curve at a starting concentration of 10 μM. Cells were treated with DMSO only as a negative control. Cell viability was evaluated using a tetrazolium-based assay with an EZ-Cytox Cell Viability Assay kit (No. EZ-12000; Daeil Lab Service Co. Ltd., Seoul, Korea), according to the manufacturer's protocol. After incubation for 3 h, the absorbance was measured using a Victor X5 multilabel reader (Perkin Elmer). The 50% cell growth inhibition (GI_{50}) values were calculated using nonlinear regression analysis in GraphPad Prism software 5.01 (GraphPad Software).

KM12C cells were plated in a 6-well plate at a density of 1.2×10^6 cells/well in 2 mL medium overnight. The monolayer of cells was wounded by scraping with a pipette tip and washed gently with phosphate-buffered saline (PBS) to remove the detached cells. The cells were subsequently treated with the indicated concentrations of KRC-108. Wounds were imaged at 0 and 24 h after the scratch under a light microscope (magnification, ×100; Axiovert 200, Carl Zeiss AG, Jena, Germany). The wound area that recovered over 24 h was measured using ImageJ software (National Institute of Health, Bethesda, MD, USA).

Drug combination analysis

The cells were plated at a density of 2,000 cells/well and allowed to adhere overnight. A concentration range of 0.195-100 μM was used for 5-fluorouracil (5-FU) and KRC-108 was tested in a range of 15 nM to 7.5 μM. The 5-FU and KRC-108 were mixed in a 13.3:1 ratio as calculated by the GI_{50} ratio of 5-FU (2.90 μM) and KRC-108 (220 nM), and incubated with the cells for 72 h in a humidified chamber at 37°C. After incubation, the EZ-Cytox cell viability assay was performed as described previously. Possible combinations of the two drugs within these concentration ranges were analyzed for any additive, synergistic, or antagonistic effects. The data were analyzed for combination index (Chou and Talalay, 1984) using Compusyn software (version 1.0; ComboSyn Inc., Paramus, NJ, USA).

Immunoblot analysis

Cells were lysed in sodium dodecyl sulfate (SDS) lysis buffer, and protein concentrations were measured using the SMART BCA Protein Assay kit (iNtRON Biotechnology, Seongnam, Korea). Samples were resolved by SDS-polyacrylamide gel electrophoresis (10%-15% acrylamide) and transferred to polyvinylidene difluoride membranes (EMD Millipore, Billerica, MA, USA). Next, the membranes were blocked with 5% nonfat milk or 5% BSA and incubated overnight with specific

primary antibodies. Antibodies against phospho-TrkA (Tyr490; #9141; 1:1000), cyclin D1 (#2922), phospho-Akt (Ser473; #9271; 1:1000), phospho-p44/42 MAPK (ERK1/2; #4370; 1:1000), phospho-PLCγ1 (Tyr783; #2821; 1:1000), PARP (#9542; 1:1000), and LC3A/B (D3U4C; #12741; 1:1000) were purchased from Cell Signaling Technology (Danvers, MA, USA). Anti-TrkA (sc-7268; 1:1000) and anti-ERK1/2 (sc-135900; 1:1000) were purchased from Santa Cruz Biotechnology (Dallas, TX, USA). β-actin (Sigma-Aldrich, St. Louis, MO, USA, #5441; 1:5000) was used as a loading control. On the following day, the membranes were washed with 1X TBST buffer and incubated in blocking buffer with goat anti-rabbit IgG (Jackson Laboratory, Bar Harbor, ME, USA, 111-035-003; 1:5000) or goat anti-mouse IgG (Jackson Laboratory; 115-035-003; 1:5000) secondary antibodies for 1 h at 22°C. Subsequently, the membranes were washed with 1X TBST buffer, and immunoblot signals were detected using the ECL Select western blotting detection reagent (Amersham ECL Select; GE Healthcare, London, UK).

Flow cytometric analysis

Cells were plated in 100 mm dish (5×10^6 cells) and incubated overnight. After incubation, the cells were treated with different concentrations of KRC-108 (0, 0.01, 0.1, 1, or 10 μM) for 24 h. The cells were then detached, fixed, treated with RNase A (50 μg/mL), and stained with propidium iodide (PI; Sigma-Aldrich). Cell cycle distribution was analyzed by flow cytometry using a BD FACSVerse™ flow cytometer (BD, Franklin Lakes, NJ, USA). The percentage of cells in different phases of the cell cycle was determined using BD FACSuite™ software (BD).

Autophagy

pAdCMV/V5-DEST-GFP-LC3B (Ad-GFP-LC3) is an adenovirus vector constructed to express the GFP-LC3 fusion protein and is used to monitor autophagy flux. The virus particles expressing GFP-LC3 proteins (Ad LC3-GFP) were kindly provided by Dr. Young-Sool Hah (Noh *et al*., 2016). Autophagosome vesicles were visualized in KM12C cells plated in 6-well plates at a density of 7×10^5 cells/well. The cells were incubated in MEM containing 10% FBS for 24 h and then transduced with Ad LC3-GFP for 24 h. After transduction, the cells were treated with DMSO or 10 μM KRC-108 for 8 h. Images were analyzed using a fluorescence microscope (Zeiss Axio Observer Z1; Carl Zeiss AG).

Mouse tumor xenograft

Animal experiments were approved by the Institutional Animal Care and Use Committee of the Korea Institute of Toxicology and conducted according to the guidelines of the Association for Assessment and Accreditation of Laboratory Animal Care International (approval number 2004-0003). A total of 1×10^7 KM12C cells were suspended in 200 μl of PBS/matrigel (1:1) and subcutaneously inoculated into the flanks of female BALB/c nu/nu (athymic nude) mice. When the tumor volume reached 100 mm^3, the mice were randomly divided into three groups (n=8 each) and administered 40 mg/kg or 80 mg/kg KRC-108 in PBS or pure PBS by oral gavage. The drug or pure PBS was administered daily for 14 days. Tumor sizes were measured twice a week for 14 days, and tumor volumes were calculated using the following formula:

$$V = \frac{XD^2}{2},$$

where V is the volume (mm^3), X is the length (mm), and D is the width of the tumor (mm). After 21 days, the mice were sacrificed, and the tumor weights (mg) were measured.

RESULTS

Inhibition of TrkA kinase activity by KRC-108

First, we tested the TrkA-inhibitory activity of KRC-108. The *in vitro* kinase activity of the recombinant TrkA protein was measured in the presence of KRC-108 (Fig. 1A). Using the TR-FRET method, the inhibition of TrkA kinase by KRC-108 was assessed, and the IC_{50} was calculated as 43.3 nM. The inhibition of TrkA by KRC-108 was further confirmed using a cell-based assay. As KM12C colon cancer cells harbor the *TPM3-NTRK1* fusion gene, the TrkA fusion protein is activated without ligand stimulation (Ardini *et al*., 2014; Medico *et al*., 2015). Based on these characteristics, KM12C cells have been used in preclinical research for TrkA-driven human colon cancer (Doebele *et al*., 2015; Ardini *et al*., 2016; Menichincheri *et al*., 2016). The level of phosphorylated TrkA protein resulting from the gene fusion was measured following KRC-108 treatment (Fig. 1B). KRC-108 treatment reduced the phosphorylation of TrkA in a dose-dependent manner. Inhibition of TrkA phosphorylation was observed starting at a concentration of 0.1 μM KRC-108. These results indicate that KRC-108 perturbed TrkA activity both *in vitro* and in a cell-based assay.

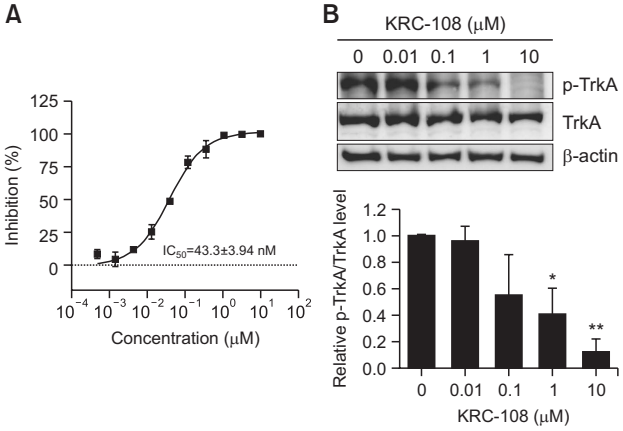

Fig. 1. Inhibition of TrkA kinase activity by KRC-108. (A) *In vitro* TrkA kinase activity was measured using the TR-FRET method. KRC-108 was used at the indicated concentrations. The kinase activity of recombinant TrkA protein was measured and the % inhibition was calculated, compared to DMSO control. Data are presented as the means ± standard error of mean (SEM) of three independent experiments. (B) KM12C cells were treated with KRC-108 at the indicated concentrations and were subjected to western blot analyses. TrkA phosphorylation was measured using antibodies against phosphorylated TrkA (p-TrkA) and TrkA. β-actin was used as loading control. The intensity of the bands was quantified using densitometry. The relative level of p-TrkA vs TrkA was calculated and indicated in the graph. The symbols * and ** indicate $p<0.05$ and $p<0.01$, respectively.

Inhibition of cell growth by KRC-108

KM12C colon cancer cells were subjected to a cell viability assay following treatment with KRC-108. KRC-108 exhibited potent growth inhibitory activity, with a GI_{50} of 220 nM (Fig. 2A). The effect of KRC-108 on cell growth in combination with 5-FU, a chemotherapeutic agent indicated for colon cancer patients, was investigated (Fig. 2B). First, the ratio of KRC-108 to 5-FU concentration for treatment was determined to be 1:13.3, based on the GI_{50} values of 5-FU (2.90 μM) and KRC-108 (220 nM). The combination index (CI) was calculated as 0.579 from the cell viability assay of the combination treatment, indicating a synergism between 5-FU and KRC-108 in the combined treatment. These combination treatment experiments showed that the addition of KRC-108 to a 5-FU-based regimen may be suitable for colon cancer therapy.

The effect of KRC-108 on cell migration was assessed using a wound-healing assay. Scratches were made to the cell monolayer, and cells were allowed to migrate into the wounds for 24 h in the absence and presence of KRC-108. In the absence of KRC-108, cells migrated and filled the gap in the scratches, whereas KRC-108 treatment suppressed cell migration in a dose-dependent manner (Fig. 2C). A total of 41.8% of the wound area was recovered following the migration of cells for 24 h without drug treatment. Only 31.2% and 17.2% of the wound area was recovered with treatments of 1 μM and 10 μM KRC-108, respectively.

Effect of KRC-108 on cell cycle and apoptosis

Given the growth inhibitory effects of KRC-108, we next examined its effects on cell cycle progression. KM12C cells were treated with various concentrations of KRC-108 for 24 h and then subjected to cell cycle analysis. The cell population in the G1 phase increased from 66.6% (DMSO control) to 77.0% (1 μM KRC-108), indicating G1 phase arrest (Fig. 3). Consistent with this cell cycle arrest, the level of cyclin D1 decreased following treatment with KRC-108 concentrations >0.1 μM.

To examine the effect of KRC-108 on apoptosis as a means of suppressing cell growth, PARP cleavage was assessed (Fig. 3C). A slight increase in cleaved PARP was observed in cells following treatment with >1 μM KRC-108. These results indicate that both cell cycle arrest and apoptotic cell death contribute to KRC-108-mediated growth inhibition.

Effect of KRC-108 on autophagy

To evaluate the phenotypic changes induced by KRC-108, we analyzed the morphological changes in cells following KRC-108 treatment. As shown in Fig. 4A (right panel), increased vacuole formation was observed in KRC-108-treated cells. These appeared to be autophagic vacuoles and were further confirmed using the LC3 puncta assay and western blotting. LC3 protein, a marker of autophagy, was found to be induced following treatment with 10 μM KRC-108 (Fig. 4B). The formation of LC3 puncta by KRC-108 was also visualized using GFP-LC3 (Fig. 4A). These results suggest that KRC-

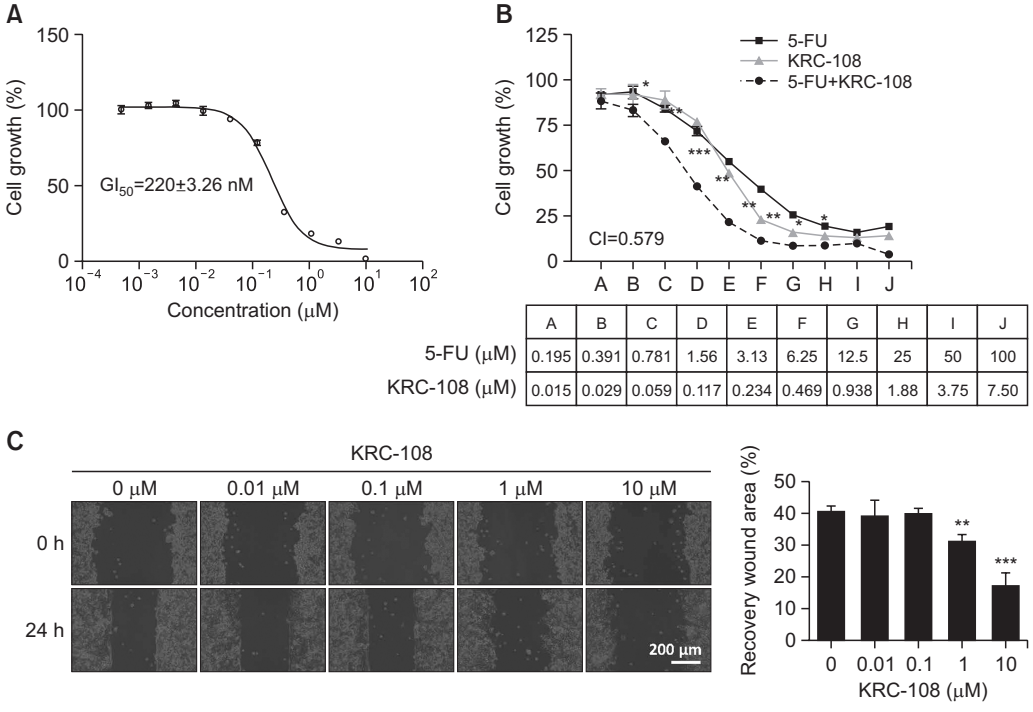

	A	B	C	D	E	F	G	H	I	J
5-FU (μM)	0.195	0.391	0.781	1.56	3.13	6.25	12.5	25	50	100
KRC-108 (μM)	0.015	0.029	0.059	0.117	0.234	0.469	0.938	1.88	3.75	7.50

Fig. 2. Growth suppression by KRC-108. (A) KM12C cells were treated with KRC-108 at the indicated concentration for 72 h, and cell growth was measured using EZ-Cytox Cell Viability Assay kit. Data are presented as the mean ± SEM of three independent experiments. (B) Cells were treated with KRC-108, 5-fluorouracil (5-FU), or a combination of KRC-108 and 5-FU (ratio 1:13.3) for 72 h. Cell growth was determined using a cell viability assay and the combination index was calculated using CompuSyn software (CI value >1.0, antagonism; CI value=1.0, additivity; CI value< 1.0, synergism). The data are the mean ± SEM of three independent experiments. (C) Cell migration was measured using a wound healing assay. Cells were grown in a monolayer and scratched, then were treated with KRC-108 at the indicated concentration for 24 h. Cell migration was observed under a phase contrast microscope. Wound area following a 24 h recovery was quantified using ImageJ software and indicated in the graph. The symbols *, **, and *** indicate $p<0.05$, $p<0.01$, and $p<0.001$, respectively.

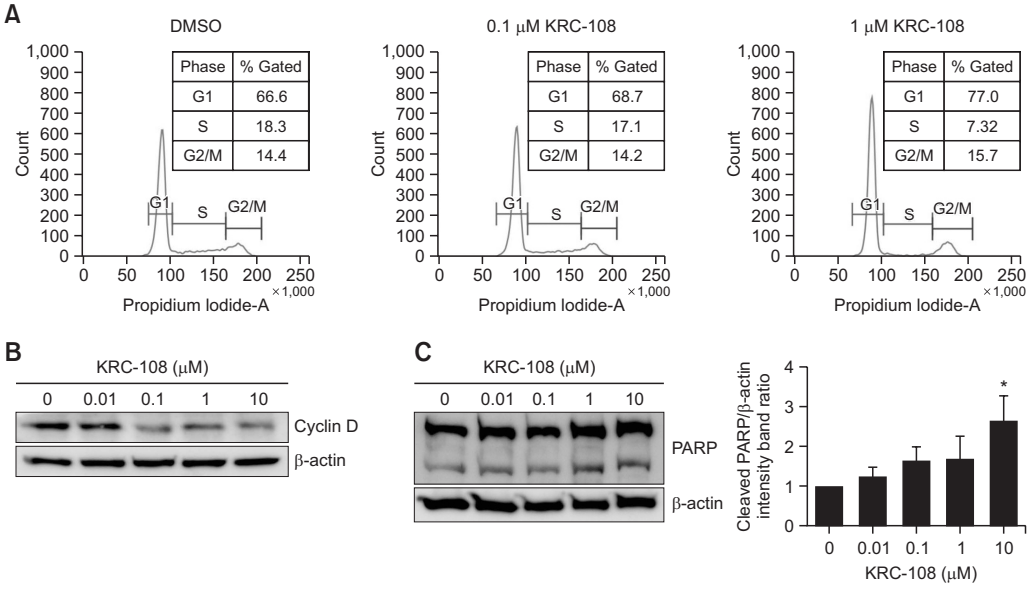

Fig. 3. Effect of KRC-108 on the cell cycle. (A) KM12C cells were treated with KRC-108 at the indicated concentrations for 24 h and subjected to cell cycle analyses. (B) Cells were treated with KRC-108 at the indicated concentration for 48 h, and then subjected to western blot analysis using an antibody against cyclin D. (C) Cells were treated with KRC-108 at the indicated concentration for 24 h, and then subjected to western blot analysis using an antibody against PARP. Immunoblot analysis of β-actin was used as the loading control. The intensity of the bands was quantified using densitometry. The relative level of cleaved PARP vs β-actin was calculated and indicated in the graph. The symbol * indicates $p<0.05$.

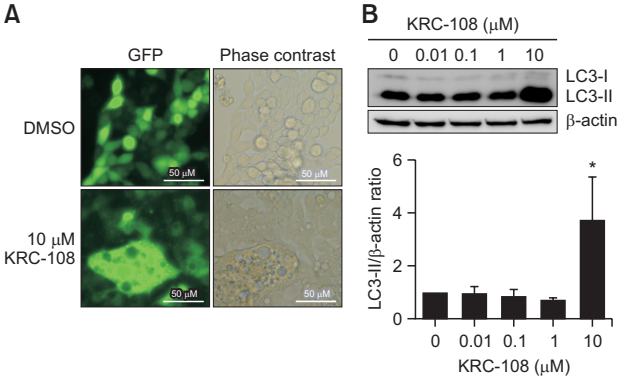

Fig. 4. Effect of KRC-108 on autophagy. (A) KM12C cells were transiently transfected with GFP-LC3 for 24 h, and then treated with DMSO or 10 μM KRC-108 for 8 h. GFP-LC3 puncta were examined by fluorescence microscopy. (B) Endogenous LC3 was detected in KM12C cells treated with KRC-108 for 24 h by immunoblotting with an anti-LC3 antibody. β-actin was used as a loading control. The intensity of the bands was quantified using densitometry. The relative level of LC3-II vs β-actin was calculated and indicated in the graph. The symbol * indicates $p<0.05$.

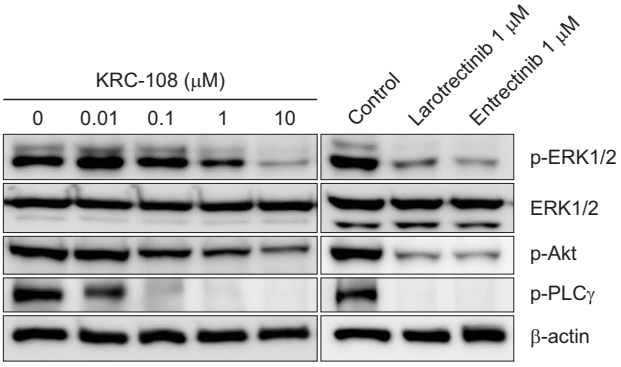

Fig. 5. Effect of KRC-108 on the TrkA signaling pathway. Cells were treated with KRC-108 at the indicated concentrations for 24 h. Western blotting was then performed using the indicated antibodies. The immunoblot images are representative of three independent experiments.

108 causes an increase in the number of autophagosomes in cells.

Effect of KRC-108 on TrkA signaling

Next, TrkA-regulated downstream signaling molecules were examined in the presence of KRC-108 (Fig. 5). Phosphorylated TrkA transduces signals and activates ERK1/2, Akt, and PLCγ via phosphorylation. Phosphorylation of the downstream signaling molecules was reduced following KRC-108 treatment. A slight reduction in phosphorylation level was observed following treatment with 0.1 μM KRC-108, whereas a sharp decrease in phosphorylation was observed in cells treated with 1 μM and 10 μM KRC-108. Phosphorylated PLCγ was completely undetectable in cells treated with 1 μM and 10 μM KRC-108. These results concerning the activation of downstream signaling molecules are consistent with KRC-108-mediated inhibition of TrkA activity, as shown in Fig. 1.

In vivo anti-tumor effect of KRC-108

The *in vivo* anti-tumor effect of KRC-108 was analyzed using a xenograft model. Xenografts were generated by inoculating KM12C cells into BALB/c *nu/nu* mice, followed by

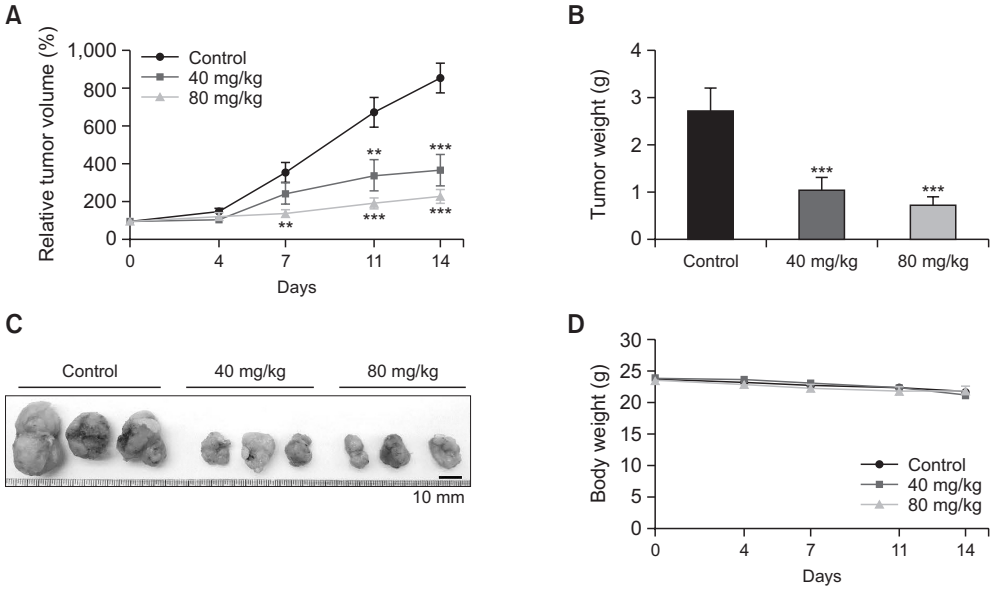

Fig. 6. *In vivo* anti-tumor efficacy of KRC-108. Tumor xenografts were generated by inoculating KM12C cells into BALB/c *nu/nu* mice and allowing the tumors to grow to the size of 100 mm^3. KRC-108 or a PBS control was administered to the mice at 40 mg/kg or 80 mg/kg, respectively, by oral gavage for 14 days. (A) Tumor size was measured on the indicated days following the start of drug administration. Tumor volume was calculated using the formula: V (volume)=X (length)×D (width)^2/2. (B) Tumor xenografts were isolated, and the tumors were weighed on day 14. (C) Photographic images of representative tumors are shown. (D) Mice body weights were measured on the indicated days. Results represent the mean ± SEM. The symbols ** and *** indicate p<0.01 and p<0.001, respectively.

administration of KRC-108 compound by oral gavage. Treatment with 40 mg/kg and 80 mg/kg KRC-108 along with a PBS control treatment were carried out for 14 days, and tumor size was measured on days 7 and 14. As shown in Fig. 6A, KRC-108 inhibited xenograft growth in a dose-dependent manner. A total of 73.0% inhibition of tumor growth was observed on day 14 in the 80 mg/kg KRC-108-treated group.

Upon completion of treatment, the tumor mass was dissected from *nu/nu* mice and weighed. Treatment with KRC-108 reduced tumor weight and tumor size in a dose-dependent manner (Fig. 6B). Fig. 6C shows representative tumors dissected from the PBS control, 40 mg/kg KRC-108, and 80 mg/kg KRC-108 groups. No significant changes in body weight were observed during the 14 days of drug administration (Fig. 6D). The *in vivo* effects of KRC-108 observed in this experiment, along with the *in vitro* effects of KRC-108 on colon cancer cell lines, confirmed its potential as an anti-tumor agent.

DISCUSSION

The Trk signaling pathway is a therapeutic target for pain management and cancer (Hirose *et al*., 2016). The occurrence of *NTRK* fusion genes in cancer patients led to the development of Trk inhibitors as anticancer agents, whereas the development of TrkA inhibitors as analgesics is based on the discovery of NGF-induced pain. Two anticancer drugs targeting Trk, larotrectinib and entrectinib, are indicated for cancers involving TRK fusion proteins, regardless of tumor type (Al-Salama and Keam, 2019; Scott, 2019). This type of therapy, which uses drugs to treat cancers based on the genetic signature of the cancer independent of cancer type, is called tissue-agnostic therapy (Jorgensen, 2020). Along with larotrectinib and entrectinib, pembrolizumab and dostarlimab are tissue-agnostic drugs that have received FDA approval.

KRC-108 was previously reported as a multi-kinase inhibitor, mainly targeting c-Met, Flt3, and ALK (Han *et al*., 2012). It has also been reported to act as an Aurora A inhibitor with anti-tumor activity against colon cancer cells (Chung *et al*., 2015). The TrkA-inhibitory activity of KRC-108 was relatively potent in the present study, with an IC_{50} of 43.3 nM (Fig. 1), whereas the IC_{50} for c-Met, Flt3, ALK, and Aurora A were 80, 30, 780, and 590 nM, respectively. Further characterization of KRC-108 as a TrkA inhibitor was performed in this study. Although the growth inhibitory effects of KRC-108 on the HT-29 colon cancer cell line were determined in previous reports, colon cancer cells expressing Trk fusion protein have not been evaluated. Given that larotrectinib and entrectinib were developed as tissue-agnostic therapies to specifically target Trk fusion positive cancers, we investigated the specific targeting of KRC-108 to Trk fusion positive cancer cells in this study.

Treatment with KRC-108 induced autophagy, apoptosis, and cell cycle arrest in KM12C cells (Fig. 3, 4). Several kinase inhibitors have been reported to activate autophagy, including imatinib, sorafenib, crizotinib, pazopanib, and sunitinib (Pan *et al*., 2014). Activation of autophagy generally promotes cell survival, thus contributing to cancer drug resistance (Onorati *et al*., 2018). Therefore, inhibition of autophagy has emerged as a promising approach for the development of anticancer agents and sensitizers for anticancer drugs (Levy *et al*., 2017). Given the role of autophagy in cancer, KRC-108-induced autophagy may have a negative effect on the growth suppressive effects of KRC-108. Autophagy is negatively regulated by the PI3K/Akt pathway via the activation of mTOR (Kondo *et al*., 2005). Inhibition of Akt activity by KRC-108 may contribute to the induction of autophagy in KM12C cells (Fig. 5).

Reports have suggested a relationship between autophagy and TrkA-overexpressing cells. Overexpression of TrkA in neuronal SK-N-MC or non-neuronal USOS cells resulted in cell death associated with autophagy (Dadakhujaev *et al*., 2008, 2009). Another group also reported autophagic cell death of glioblastoma cell lines by TrkA activation (Hansen *et al*., 2007). In contrast to the results of this study that indicated autophagy induction by TrkA inhibitors, TrkA activation was found to induce autophagic cell death in previous studies. Thus, the role of TrkA in autophagy may be context-dependent and cell-type dependent.

TrkA transduces signals via Akt, ERK1/2, and PLCγ for neuronal survival and differentiation. Downstream signaling effectors of TrkA fusion proteins appear to be the same as those of the wild-type TrkA protein. In the case of the *TPM3-NTRK1* fusion found in the KM12C cells used in this study, the binding sites required for Akt, ERK1/2, and PLCγ signaling are present in the fusion protein (Cocco *et al*., 2018). The Y496 and Y791 autophosphorylation sites of TrkA are docking sites required for downstream signaling (Reichardt, 2006), and the corresponding tyrosine residues of TPM3-TrkA appear to function as docking sites for signaling effector molecules. As shown in Fig. 5, KRC-108 suppressed signal transduction to these three major signal transduction pathways. Phosphorylation of ERK1/2, Akt, and PLCγ was reduced following treatment with KRC-108 in a dose-dependent manner. In addition, inhibition of ERK1/2, Akt, and PLCγ phosphorylation was consistent with the induction of apoptosis by KRC-108 (Fig. 3C) (Franke *et al*., 2003; Cagnol and Chambard, 2010).

The prevalence of NTRK fusion in malignancies has been previously investigated using the Cancer Genome Atlas database (Okamura *et al*., 2018). Only 0.31% of adult tumor samples presented an NTRK fusion, indicating that this alteration is an exceedingly rare event. The highest incidence of NTRK fusion was observed in thyroid cancer (2.34%, 12 out of 513 samples), and 0.97% of colon adenocarcinomas (3 out of 310 samples) carried the *NTRK* fusion gene. This low prevalence of NTRK alteration may be an obstacle in recruiting patients with NTRK fusion in a clinical trial. This can be overcome by adopting the tissue-agnostic approach. Clinical studies for testing the efficacy and safety of Trk inhibitors may be performed using other tumor types containing the same NTRK fusion biomarker.

The results of this study suggest that KRC-108 is a promising small molecule for therapeutic application in cancers with TrkA fusion. Investigation of TrkA inhibitors such as KRC-108 compound will accelerate advances in tissue-agnostic agents and precision medicine. Identification of TrkA fusions in various types of cancers, and diagnostic techniques for the identification of chromosomal rearrangements and mutations in cancer patients should be accompanied by the development of TrkA-targeting agents.

CONFLICT OF INTEREST

The authors declare that they have no conflict of interests.

ACKNOWLEDGMENTS

This research was funded by the National Research Foundation, Government of Korea, grant number 2021R1A2C1007790 (S-Y.H.) and 2021R1A2C2010431 (J.L.).

REFERENCES

Al-Salama, Z. T. and Keam, S. J. (2019) Entrectinib: first global approval. *Drugs* **79**, 1477-1483.

Ardini, E., Bosotti, R., Borgia, A. L., De Ponti, C., Somaschini, A., Cammarota, R., Amboldi, N., Raddrizzani, L., Milani, A., Magnaghi, P., Ballinari, D., Casero, D., Gasparri, F., Banfi, P., Avanzi, N., Saccardo, M. B., Alzani, R., Bandiera, T., Felder, E., Donati, D., Pesenti, E., Sartore-Bianchi, A., Gambacorta, M., Pierotti, M. A., Siena, S., Veronese, S., Galvani, A. and Isacchi, A. (2014) The TPM3-NTRK1 rearrangement is a recurring event in colorectal carcinoma and is associated with tumor sensitivity to TRKA kinase inhibition. *Mol. Oncol.* **8**, 1495-1507.

Ardini, E., Menichincheri, M., Banfi, P., Bosotti, R., De Ponti, C., Pulci, R., Ballinari, D., Ciomei, M., Texido, G., Degrassi, A., Avanzi, N., Amboldi, N., Saccardo, M. B., Casero, D., Orsini, P., Bandiera, T., Mologni, L., Anderson, D., Wei, G., Harris, J., Vernier, J. M., Li, G., Felder, E., Donati, D., Isacchi, A., Pesenti, E., Magnaghi, P. and Galvani, A. (2016) Entrectinib, a Pan-TRK, ROS1, and ALK inhibitor with activity in multiple molecularly defined cancer indications. *Mol. Cancer Ther.* **15**, 628-639.

Bongarzone, I., Pierotti, M. A., Monzini, N., Mondellini, P., Manenti, G., Donghi, R., Pilotti, S., Grieco, M., Santoro, M. and Fusco, A. (1989) High frequency of activation of tyrosine kinase oncogenes in human papillary thyroid carcinoma. *Oncogene* **4**, 1457-1462.

Cagnol, S. and Chambard, J.-C. (2010) ERK and cell death: mechanisms of ERK-induced cell death – apoptosis, autophagy and senescence. *FEBS J.* **277**, 2-21.

Cho, S. Y., Han, S. Y., Ha, J. D., Ryu, J. W., Lee, C. O., Jung, H., Kang, N. S., Kim, H. R., Koh, J. S. and Lee, J. (2010) Discovery of aminopyridines substituted with benzoxazole as orally active c-Met kinase inhibitors. *Bioorg. Med. Chem. Lett.* **20**, 4223-4227.

Chou, T. C. and Talalay, P. (1984) Quantitative analysis of dose-effect relationships: the combined effects of multiple drugs or enzyme inhibitors. *Adv. Enzyme Regul.* **22**, 27-55.

Chung, H. J., Park, K. R., Lee, H. J., Lee, J., Kim, J. H., Kim, Y. C. and Han, S. Y. (2015) Effects of KRC-108 on the Aurora A activity and growth of colorectal cancer cells. *Biochem. Biophys. Res. Commun.* **461**, 605-611.

Cocco, E., Scaltriti, M. and Drilon, A. (2018) NTRK fusion-positive cancers and TRK inhibitor therapy. *Nat. Rev. Clin. Oncol.* **15**, 731-747.

Dadakhujaev, S., Jung, E. J., Noh, H. S., Hah, Y. S., Kim, C. J. and Kim, D. R. (2009) Interplay between autophagy and apoptosis in TrkA-induced cell death. *Autophagy* **5**, 103-105.

Dadakhujaev, S., Noh, H. S., Jung, E. J., Hah, Y.-S., Kim, C. J. and Kim, D. R. (2008) The reduced catalase expression in TrkA-induced cells leads to autophagic cell death via ROS accumulation. *Exp. Cell Res.* **314**, 3094-3106.

Doebele, R. C., Davis, L. E., Vaishnavi, A., Le, A. T., Estrada-Bernal, A., Keysar, S., Jimeno, A., Varella-Garcia, M., Aisner, D. L., Li, Y., Stephens, P. J., Morosini, D., Tuch, B. B., Fernandes, M., Nanda, N. and Low, J. A. (2015) An oncogenic NTRK fusion in a patient with soft-tissue sarcoma with response to the tropomyosin-related kinase inhibitor LOXO-101. *Cancer Discov.* **5**, 1049-1057.

Doebele, R. C., Drilon, A., Paz-Ares, L., Siena, S., Shaw, A. T., Farago, A. F., Blakely, C. M., Seto, T., Cho, B. C., Tosi, D., Besse, B., Chawla, S. P., Bazhenova, L., Krauss, J. C., Chae, Y. K., Barve, M., Garrido-Laguna, I., Liu, S. V., Conkling, P., John, T., Fakih, M., Sigal, D., Loong, H. H., Buchschacher, G. L., Jr., Garrido, P., Nieva, J., Steuer, C., Overbeck, T. R., Bowles, D. W., Fox, E., Riehl, T., Chow-Maneval, E., Simmons, B., Cui, N., Johnson, A., Eng, S., Wilson, T. R. and Demetri, G. D.; trial investigators (2020) Entrectinib in patients with advanced or metastatic NTRK fusion-positive solid tumours: integrated analysis of three phase 1-2 trials. *Lancet Oncol.* **21**, 271-282.

Franke, T. F., Hornik, C. P., Segev, L., Shostak, G. A. and Sugimoto, C. (2003) PI3K/Akt and apoptosis: size matters. *Oncogene* **22**, 8983-

8998.
Han, S. Y. (2021) TRK Inhibitors: tissue-agnostic anti-cancer drugs. *Pharmaceuticals (Basel)* **14**, 632.
Han, S. Y., Lee, C. O., Ahn, S. H., Lee, M. O., Kang, S. Y., Cha, H. J., Cho, S. Y., Ha, J. D., Ryu, J. W., Jung, H., Kim, H. R., Koh, J. S. and Lee, J. (2012) Evaluation of a multi-kinase inhibitor KRC-108 as an anti-tumor agent *in vitro* and *in vivo*. *Invest. New Drugs* **30**, 518-523.
Hansen, K., Wagner, B., Hamel, W., Schweizer, M., Haag, F., Westphal, M. and Lamszus, K. (2007) Autophagic cell death induced by TrkA receptor activation in human glioblastoma cells. *J. Neurochem.* **103**, 259-275.
Harada, G., Gongora, A. B. L., da Costa, C. M. and Santini, F. C. (2020) TRK inhibitors in non-small cell lung cancer. *Curr. Treat. Options Oncol.* **21**, 39.
Hirose, M., Kuroda, Y. and Murata, E. (2016) NGF/TrkA signaling as a therapeutic target for pain. *Pain Pract.* **16**, 175-182.
Jorgensen, J. T. (2020) Site-agnostic biomarker-guided oncology drug development. *Expert Rev. Mol. Diagn.* **20**, 583-592.
Khotskaya, Y. B., Holla, V. R., Farago, A. F., Mills Shaw, K. R., Meric-Bernstam, F. and Hong, D. S. (2017) Targeting TRK family proteins in cancer. *Pharmacol. Ther.* **173**, 58-66.
Kondo, Y., Kanzawa, T., Sawaya, R. and Kondo, S. (2005) The role of autophagy in cancer development and response to therapy. *Nat. Rev. Cancer* **5**, 726-734.
Levy, J. M. M., Towers, C. G. and Thorburn, A. (2017) Targeting autophagy in cancer. *Nat. Rev. Cancer* **17**, 528-542.
Martin-Zanca, D., Hughes, S.H. and Barbacid, M. (1986) A human oncogene formed by the fusion of truncated tropomyosin and protein tyrosine kinase sequences. *Nature* **319**, 743-748.
Medico, E., Russo, M., Picco, G., Cancelliere, C., Valtorta, E., Corti, G., Buscarino, M., Isella, C., Lamba, S., Martinoglio, B., Veronese, S., Siena, S., Sartore-Bianchi, A., Beccuti, M., Mottolese, M., Linnebacher, M., Cordero, F., Di Nicolantonio, F. and Bardelli, A. (2015) The molecular landscape of colorectal cancer cell lines unveils clinically actionable kinase targets. *Nat. Commun.* **6**, 7002.
Menichincheri, M., Ardini, E., Magnaghi, P., Avanzi, N., Banfi, P., Bossi, R., Buffa, L., Canevari, G., Ceriani, L., Colombo, M., Corti, L., Donati, D., Fasolini, M., Felder, E., Fiorelli, C., Fiorentini, F., Galvani, A., Isacchi, A., Borgia, A. L., Marchionni, C., Nesi, M., Orrenius, C., Panzeri, A., Pesenti, E., Rusconi, L., Saccardo, M. B., Vanotti, E., Perrone, E. and Orsini, P. (2016) Discovery of entrectinib: a new 3-aminoindazole as a potent anaplastic lymphoma kinase (ALK), c-ros oncogene 1 kinase (ROS1), and pan-tropomyosin receptor kinases (pan-TRKs) inhibitor. *J. Med. Chem.* **59**, 3392-3408.
Noh, H. S., Hah, Y. S., Zada, S., Ha, J. H., Sim, G., Hwang, J. S., Lai, T. H., Nguyen, H. Q., Park, J. Y., Kim, H. J., Byun, J. H., Hahm, J. R., Kang, K. R. and Kim, D. R. (2016) PEBP1, a RAF kinase inhibitory protein, negatively regulates starvation-induced autophagy by direct interaction with LC3. *Autophagy* **12**, 2183-2196.
Okamura, R., Boichard, A., Kato, S., Sicklick, J. K., Bazhenova, L. and Kurzrock, R. (2018) Analysis of NTRK alterations in pan-cancer adult and pediatric malignancies: implications for NTRK-targeted therapeutics. *JCO Precis. Oncol.* **2018**, PO.18.00183.
Onorati, A. V., Dyczynski, M., Ojha, R. and Amaravadi, R. K. (2018) Targeting autophagy in cancer. *Cancer* **124**, 3307-3318.
Pan, H., Wang, Z., Jiang, L., Sui, X., You, L., Shou, J., Jing, Z., Xie, J., Ge, W., Cai, X., Huang, W. and Han, W. (2014) Autophagy inhibition sensitizes hepatocellular carcinoma to the multikinase inhibitor linifanib. *Sci. Rep.* **4**, 6683.
Reichardt, L. F. (2006) Neurotrophin-regulated signalling pathways. *Philos. Trans. R. Soc. Lond. B Biol. Sci.* **361**, 1545-1564.
Scott, L. J. (2019) Larotrectinib: first global approval. *Drugs* **79**, 201-206.